HHS Public Access

Author manuscript

Circ Res. Author manuscript; available in PMC 2020 January 04.

Published in final edited form as:

Circ Res. 2019 January 04; 124(1): 101–113. doi:10.1161/CIRCRESAHA.118.313835.

Adrenomedullin Induces Cardiac Lymphangiogenesis After Myocardial Infarction and Regulates Cardiac Edema Via Cx43

Claire E. Trincot[1], **Wenjing Xu**[2], **Hua Zhang**[2], **Molly R. Kulikauskas**[2], **Thomas G. Caranasos**[3], **Brian C. Jensen**[4,5,6], **Amelie Sabine**[7], **Tatiana V. Petrova**[7,8], and **Kathleen M. Caron**[1,6,9]

[1]Curriculum in Genetics and Molecular Biology, University of North Carolina at Chapel Hill [2]Department of Cell Biology and Physiology, University of North Carolina at Chapel Hill [3]Department of Surgery, Division of Cardiothoracic Surgery, University of North Carolina at Chapel Hill [4]Division of Cardiology, University of North Carolina at Chapel Hill [5]Department of Medicine, School of Medicine, University of North Carolina at Chapel Hill [6]McAllister Heart Institute, University of North Carolina at Chapel Hill [7]Department of Oncology, University of Lausanne and Lausanne University Hospital and Ludwig Institute for Cancer Research Lausanne, Chemin de Boveresses 155, CH-1066, Switzerland [8]Division of Experimental Pathlogy, Lausanne University Hospital [9]Department of Cell Biology and Physiology, University of North Carolina at Chapel Hill kathleen_caron@med.unc.edu, 111 Mason Farm Rd, MBRB 6312B, CB 7545, Chapel Hill, NC 27599

Abstract

Rationale: Cardiac lymphangiogenesis contributes to the reparative process post myocardial infarction (MI), but the factors and mechanisms regulating it are not well understood.

Objective: To determine if epicardial-secreted factor adrenomedullin (AM=protein; *Adm*=gene) improves cardiac lymphangiogenesis post-MI via lateralization of Connexin43 (Cx43) in cardiac lymphatic vasculature.

Methods and Results: Firstly, we identified sex-dependent differences in cardiac lymphatic numbers in uninjured mice using light sheet microscopy. Using a mouse model of Adm overexpression ($Adm^{hi/hi}$) and permanent left anterior descending (LAD) ligation to induce MI, we investigated cardiac lymphatic structure, growth, and function in injured murine hearts. Overexpression of *Adm* increased lymphangiogenesis and cardiac function post-MI while suppressing cardiac edema and correlated with changes in Cx43 localization. Lymphatic function in response to AM treatment was attenuated in mice with a lymphatic-specific Cx43 deletion. *In vitro* experiments in cultured human lymphatic endothelial cells (hLECs) identified a novel mechanism to improve gap junction coupling by pharmaceutically targeting Cx43 with verapamil.

Address correspondence to: Dr. Kathleen M. Caron, Department of Cell Biology and Physiology, University of North Carolina at Chapel Hill, 111 Mason Farm Rd, MBRB 6312B, CB 7545, Chapel Hill, NC 27599, kathleen_caron@med.unc.edu.

DISCLOSURES

None.

Finally, we show that connexin protein expression in cardiac lymphatics is conserved between mouse and human.

Conclusions: AM is an endogenous, epicardial-derived factor that drives reparative cardiac lymphangiogenesis and function via Cx43, and this represents a new therapeutic pathway for improving myocardial edema after injury.

Keywords

Cardiac; lymphatics; adrenomedullin; Cx43; edema

Subject Terms

Echocardiography; Myocardial Infarction; Physiology; Remodeling

INTRODUCTION

Lymphatic vascular circulation is essential for maintaining fluid dynamics, immune responses, and fat absorption. Defects in any aspect of lymphatic development or function can have dire effects in almost every organ system and in a large breadth of disease and injuries[1, 2]. The heart has its own unique system of lymphatic vasculature consisting of an interconnected network of vessels covering the epicardial and sub-epicardial surface most densely concentrated surrounding the ventricles of the heart [3]. Cardiac lymphatics maintain the fluid homeostasis and immune response within the cardiovascular system [4, 5]. Failure of these vessels to function properly and maintain a normal endothelial barrier can have profound consequences resulting in hypertension, inflammation, fibrosis, edema, and hemorrhage [6–8]. Recent work suggests a re-activation of these vessels following myocardial infarction (MI) may be the key to repair and scar tissue prevention by increasing cardiac function and prolonging survival [9–11]. However, precise factors that are endogenously expressed and induced following MI to drive this process remain to be elucidated.

Adrenomedullin (AM=protein; *Adm*=gene), a known cardioprotective peptide, is essential for proper cardiovascular and lymphatic development in mice[12]. In murine studies, AM can stabilize the lymphatic endothelial barrier[13]. AM is clinically significant as well. In a pilot study, patients with acute MI received intravenous AM treatment and showed significant cardiovascular improvement[14]. Additionally, the BACH (Biomarkers in Acute Heart Failure) study and The Interdisciplinary Network Heart Failure (INH) program showed that mid-regional pro-adrenomedullin (MR-proAM), a cleaved form of AM, proved an effective diagnostic and prognostic tool and may be more sensitive than traditional biomarkers like natriuretic peptides in identifying high-risk patients[15, 16]. Although the upregulation of AM in disease states is well-appreciated, the downstream effectors and mechanism of action remain only partially understood[17].

Cardiomyocytes must make connections with adjacent cells for communication of electrical impulses and propagation of contractions within the myocardium. Connexin 43 (Cx43) is the most abundantly expressed connexin within the heart and is essential for normal cardiac conductivity[18]. Typically, six connexins oligomerize to form an opening or pore in the cell

membrane known as a hemichannel [19]. When two hemichannels from adjacent cells oppose one another, they form a connection that links the cytoplasm of those two cells, known as a gap junction, named for the steric 2–3nm "gap" that forms between cells at this junction [20]. Gap junction intercellular communication (GJIC) allows for the passage of small signaling molecules, ions, metabolites, ATP, prostaglandins, small peptides, miRNAs, etc. to pass from one cell to another [21–23]. Given the role of Cx43 in cardiomyocyte contractility and cell-cell coupling, it has been highlighted as a potential therapeutic target[24–26]. Connexins and gap junctions are also critical in the proper development and maintenance of lymphatic function[27]. Lymphatic deletion of Cx43 leads to a delay in lymphatic valve initiation, improper lymphatic valve formation and function, altered lymphatic capillary patterning, and sometimes lethal chylothorax [28]. Not only are connexins vital to proper lymphatic development, but they may affect mature lymphatics through paracrine signaling via hemichannels and GJIC [29]. Human mutations in connexin proteins lead to a variety of lymphatic disorders including lymphedema[30–32].

Although connexin proteins have been studied extensively within the context of cardiomyocytes and electrical conduction in the heart, there has been little work done to evaluate how connexins specifically contribute to the function and maintenance of cardiac lymphatic vasculature. For the first time, we characterize connexin protein expression patterns within the cardiac lymphatic vasculature both in murine and human heart tissue. In this study, we demonstrate a critical role for AM in lymphangiogenesis in the heart and how it may regulate Cx43 in cardiac lymphatics to improve cardiac function after MI.

METHODS

The authors declare that all supporting data are available within the article and its online supplementary files.

Animals.

Adm$^{hi/hi}$ mice were designed as previously described in which the targeting vector replaces the endogenous 3' UTR to stabilize the mRNA and increase half-life thusly elevating *Adm* expression[33]. Genotyping was assessed using a standard PCR-based strategy with 3 primers: primer 1: 5′-AACCTTAC ACCTTGCTGAGACATTC-3′; primer 2: 5′-TTTATTAGGAAAGGACAGTGG GAGTG-3′; primer 3: 5′CCCACATT CGTGTCAAACGCTAC-3′. Primers 1 and 3 amplify a 760-bp wild-type allele, while primers 2 and 3 amplify a 600-bp targeted allele. Mice used in these studies were backcrossed to C57Bl6 for over nine generations. For all experiments, littermate animals or age-matched C57Bl6 wild type males were used as controls. All mice used were 3–6 months of age (n=84males; 33females). Cx43 (Gja1)- floxed (*Cx43*$^{fl/fl}$) mice[34] (JAX strain number 008039) were crossed with inducible Vegfr3-CreER (T2) mice[35] to produce *Vegfr3-CreER*^{T2}*; Cx43*$^{fl/fl}$. Cre-mediated recombination was induced by administering TAM (Sigma-Aldrich T5648) dissolved in corn oil and ethanol to mice aged 1–5 months (n=28) for 5 consecutive days at a dose of 10 μg/g intraperitoneally. Wild-type and Cx43-floxed allele PCR was determined by protocol provided by the Jackson Laboratory. Genotyping the Vegfr3-CreER (T2) allele was assessed using a standard PCR-based strategy with 2 primers:

primer 1: 5’ GGCTGGACCAATGTAAATATTG 3’ and primer 2: 5’ CATCATCGAAGCTTCACTG 3’ to amplify a 285-bp targeted allele. For all experiments, littermate animals or age-matched *Vegfr3*$^{+/+}$*; Cx43*$^{fl/fl}$ or *Vegfr3*$^{+/+}$*; Cx43*$^{fl/+}$ were used as controls. The animal study was in line with the guidelines and approved by the Office of Animal Care and Use at the University of North Carolina - Chapel Hill and complied with National Institute of Health guidelines.

MI model-permanent ligation of the left anterior descending (LAD) coronary artery.

Mice were anesthetized using ketamine (100 mg/kg, im) and xylazine (15 mg/kg, im) and rectal temperature maintained at 37 ± 0.5ºC. The trachea was cannulated with a 20 mm length of 18-gauge polyethylene tubing, followed by ventilation with a positive-pressure, constant-volume ventilator (model 845; Harvard Apparatus Co., South Natick, MA; stroke volume 200 ul, 150 strokes/min). A 3 mm left thoracotomy was performed between the third and fourth ribs to visualize the left anterior descending coronary artery (LAD). The proximal trunk of the LAD was ligated with 7–0 silk suture. The muscle and skin incisions were closed with 6–0 and 5–0 suture, respectively, buprenorphine administered (40 ug/kg, sc) and the animal gradually weaned from the respirator.

Light sheet microscopy.

Adult murine hearts were fixed and stained using the iDISCO method as previously described using rabbit anti-LYVE1 (1:500, Fitzgerald) primary antibody for 8 days and incubated with secondary donkey anti rabbit AF647 (1:200, Thermo Fisher Scientific) for 8 days[36]. Samples were imaged using the Lavision Ultramicroscope II light-sheet system. Images were acquired with Imaris software.

Echocardiography.

Conscious echocardiography was performed using VSI 2100 high frequency ultrasound (VisualSonics) as previously described[37].

Infarct and fibrosis.

Infarct size was assessed using traditional H&E histology and cardiac sections using a modified midline infarct size method as previously described[38]. Fibrotic area was measured by threshold level in Fiji and normalized to total area.

Scrape-loading dye transfer.

A confluent monolayer of hLECs was grown on coverslips. The scrape assay was performed as previously described[39].

Quantitative tail microlymphography.

Anesthetized adult *Vegfr3-CreER*^{T2}*; Cx43*$^{fl/fl}$ and control animals were injected in the tail with 10µl of a 25% FITC-Dextran (2,000,000 kDa) with a vehicle or AM peptide [10ng/µL] as previously described[13]. The flow of FITC-Dextran through dermal tail lymphatics was acquired with Leica MZ16FA dissecting stereoscope outfitted with a QImaging

Micropublisher 5.0 RTV color CCD camera for several minutes post injection using Metamorph software (Molecular Devices Corp.). Analyses were performed using Fiji.

Edema formation assay.

Anesthetized adult *Adm*$^{hi/hi}$ and control animals were injected with 10μl of [4μg/μl] of Complete Freund's Adjuvant (CFA) as previously described in one hind paw while the other paw served as a control[40]. Paw thickness was measured using calipers before CFA injection and every day after injection for 6 days.

Evans blue ear injection.

Ear lymphatic permeability was assessed as previously described[40]. Anesthesized adult *Vegfr3-CreER*^{T2}*; Cx43*$^{fl/fl}$ and control animals were injected intradermally with 3μl 0.5% Evans Blue dye (Sigma-Aldrich) in saline with a 10μl Hamilton syringe fitted with a 30 gauge needle. Images of the ears were acquired with Leica MZ16FA dissecting stereoscope outfitted with a QImaging Micropublisher 5.0 RTV color CCD camera using Metamorph software (Molecular Devices Corp.) at 0min., 5min., and 15min. after injection.

RESULTS

Sex-dependent differences in cardiac lymphatics.

Using light-sheet microscopy, a method of imaging immunolabeled large, intact organs with a sheet or plane of light in contrast to traditional point laser light and staining for the lymphatic vascular marker Lyve1, we characterized the three-dimensional structure and branching patterns of murine cardiac lymphatics (Figure 1a). Overall, the majority of the vessels appeared on the epicardial surface of the heart and densely cover both atria and ventricles. Many small capillaries branched from the larger collecting vessels. Vessels extended shallowly into the sub-epicardium and sub-endocardium but were notably absent from the myocardium of the ventricles. It has been shown that lymphatic capillary vessels exist in cardiac valve tissue, but the tissue is too opaque to visualize vessels within valves using this method[41]. To examine the vasculature further, we observed immunofluorescence of lymphatic marker Lyve1 in paraffin cross-sections through the ventricular wall (Figure 1b). Immunofluorescence staining allowed us to count individual vessels. Using this combination of techniques, we discovered sex-dependent differences in cardiac lymphatic vasculature. Regardless of genotype, female mice consistently had more lymphatic vessels within their heart (Figure 1c).

Given the distinct role of AM in cardiovascular and lymphatic development, we sought to characterize how overexpression of *Adm* affects the cardiac lymphatic vasculature in healthy adult mice. Male *Adm*$^{hi/hi}$ mice have approximately a 3-fold increase of AM in the heart compared to wild type littermates[42]. Adult male mice with overexpression of *Adm* showed no obvious differences in cardiac lymphatic anatomy or density compared to respective wild type littermates (Figure 1a,b). However, female *Adm*$^{hi/hi}$ mice have approximately a 60-fold increase of AM in the heart compared to wild type littermates[43]. This further increase in AM resulted in more cardiac lymphatic vasculature and a denser plexus of vessels in female *Adm*$^{hi/hi}$ mice compared to age-matched wild type mice (Figure 1a,b). The increase in the

number of vessels was most visible at higher magnification of the ventricular wall. Quantification of cardiac lymphatic vessels confirmed that there was no genotype difference in the number of vessels between male mice (Figure 1c). Yet, female $Adm^{hi/hi}$ mice had significantly more cardiac lymphatic vessels than their wild type counterparts (Figure 1c).

Adrenomedullin drives cardiac lymphangiogenesis in a surgical model of MI.

It is known that cardiac lymphatics proliferate and remodel in response to injury [9–11]. Since AM is primarily secreted from the epicardium, we considered that it may promote cardiac lymphangiogenesis after injury[42]. Using permanent LAD ligation, $Adm^{hi/hi}$ mice experience significantly more cardiac lymphatic growth than age-matched $Adm^{+/+}$ mice as quantified by counting all vessels positive for lymphatic marker Lyve1 15–21 days after MI in cross-sections through both ventricles (Figure 1d-f). Despite, increased numbers of cardiac lymphatic vessels by 15 days post-MI, male mice still had nearly equivalent number of vessels at 10 days post-MI (Online Figure I). Lymphatic vessels were most concentrated in the peri-infarct zone, especially in $Adm^{hi/hi}$ mice. Comparing the number of lymphatic vessels before and after LAD, we saw that $Adm^{hi/hi}$ mice have a higher rate of lymphatic growth after injury (Figure 1f). Further characterization of lymphatics in infarcted hearts using cardiac lymphatic vasculature marker Podoplanin confirmed more lymphangiogenesis in $Adm^{hi/hi}$ mice with denser clusters of lymphatic vessels near the epicardial border zone (Figure 1e). Despite female mice having more cardiac lymphatics before injury (independent of genotype), after MI, both sexes had comparable numbers of lymphatic vessels with $Adm^{hi/hi}$ mice consistently having more cardiac lymphatic vessels than $Adm^{+/+}$ mice.

Overexpression of Adm results in less edema and dilated cardiac lymphatic vasculature post-MI.

Histology revealed that cardiac edema post-MI is concentrated on the surface of the ventricles in the peri-infarct zones, and we observed significant differences in the swelling and accumulation of fluid between the epicardial and sub-epicardial layers of the heart between genotypes, most prominently in the male mice (Figure 2a). The left ventricular wall overall had less thinning areas and more preserved myocardium muscle in $Adm^{hi/hi}$ male mice. Consistent with the appearance of the cardiac lymphatics, we found significant differences in the extent of cardiac edema between genotypes in male mice. $Adm^{hi/hi}$ male mice had significantly less cardiac edema 15–21 days after injury as assessed and scored via histology (Figure 2a,b). Consistent with the number of lymphatic vessels, at 10 days after injury, male mice do not yet have significant differences in cardiac edema, nor do the circumferential areas of the vessels differ (Online Figure I). Female mice had no significant differences in cardiac edema 15 days after injury. It is possible that the acute, primary waves of edema were cleared more efficiently in female mice due to increased lymphatics during development, yet later stage edema was already stabilized. The difference we see in male mice may be residual clearing efficiency from the second wave of acute edema post-MI. Cardiac lymphatic vessels were dilated and increased in area in $Adm^{hi/hi}$ animals, both male and female, post-MI as quantified by measuring circumference of Lyve1 positive vessels in the ventricles of the heart. (Figure 2c,d). Microscopy revealed lymphatic vessels with more circular, patent lumens in $Adm^{hi/hi}$ mice compared to the thin, collapsed vessels of the age-matched wildtypes (Figure 2c). To further assess edema clearance in mice overexpressing

Adm, we injected the hindpaws of both $Adm^{hi/hi}$ and $Adm^{+/+}$ mice with CFA (Complete Freund's Adjuvant) to challenge the lymphatic vascular system with localized inflammation-induced edema. Both $Adm^{hi/hi}$ and control mice exhibited an immediate and significant increase in paw thickness within minutes of CFA injection that continued to worsen over 48 hours (Figure 2e). Overall, $Adm^{hi/hi}$ mice were significantly better at resolving edema. However, the timing of the resolution differed by sex, consistent with edema clearance in hearts post-MI. Female $Adm^{hi/hi}$ mice showed significantly less paw edema 1 day post injection, while $Adm^{hi/hi}$ male mice began to alleviate edema between 2 and 3 days post injection with significantly less edema by 6 days post injection. We observed differences in timing of resolution even in control mice; female control mice began to slowly resolve edema by 3 days post injection, while male control mice showed prolonged and exacerbated edema even 6 days post injection.

Overexpression of Adm correlates with improved cardiac function post-MI.

H&E histology and Picrosirius Red staining were used to characterize infarct size and fibrotic area 15–21 days after injury (Figure 3a,b). H&E was used to measure the infarct length normalized to total circumference (midline infarct). There was no significant difference in infarct size between genotypes in males or females (Figure 3a,c). Using H&E and Mason's Trichrome to measure infarcted area normalized to total area of the heart also showed no significant differences in infarct size (data not shown). Collagen deposition as evidenced by Picrosirius Red staining showed no significant differences in fibrotic scar tissue between genotypes in males or females (Figure 3b,d). In male mice, we observed no significant differences in infarct size or fibrotic area 10 days after injury (Online Figure I).

Despite the similarities in size of infarcted tissue, $Adm^{hi/hi}$ mice showed significantly improved cardiac function after MI. Uninjured $Adm^{hi/hi}$ mice and $Adm^{+/+}$ mice are functionally equivalent with no notable differences in either sex. Conscious echocardiography data, summarized in Tables 1 & 2, showed that ejection fraction and fractional shortening were significantly increased in $Adm^{hi/hi}$ mice 15 days after injury in males and 10 days after injury in females. Thus, the lymphangiogenesis and cardiac edema reduction seen in $Adm^{hi/hi}$ mice two weeks after injury appeared to have imparted significant improvement in the cardiac function compared to age-matched wildtype animals with the same amount of injury and damage. Overall, $Adm^{hi/hi}$ mice appear less dilated than wildtype animals. Representative M-mode echocardiograms show the dilation and remodeling post-MI in $Adm^{+/+}$ male mice (Figure 3e). These significant morphology changes observed in M-mode echocardiography were reflected in interventricular septal (IVS) and left ventricular internal diameter (LVID) measurements 15 days after injury in male mice.

Adrenomedullin affects localization of Cx43 in injured myocardium.

AM has previously been shown to regulate Cx43 in lymphatic endothelial cells (LECs)[39]. To assess the role of AM in regulating Cx43, we used immunofluorescence to evaluate levels and localization of the protein in cross-sections of healthy, uninjured myocardium in both $Adm^{hi/hi}$ and $Adm^{+/+}$ mice and saw no observable differences in the levels or expression pattern of Cx43 staining in either sex (Online Figure II). Next, we assessed how AM affects Cx43 in injured hearts. Immunofluorescence of Cx43 through cross-sections of the

ventricles revealed notable differences. $Adm^{hi/hi}$ male mice consistently had more Cx43 throughout the section than $Adm^{+/+}$ mice (Figure 5a). At higher magnification, Cx43 was heavily concentrated at the border of the ischemic injury in $Adm^{hi/hi}$ mice (Figure 5b). Co-staining with WGA (wheat germ agglutinin), a marker of cell borders, revealed that Cx43 retains expression within cell-cell contacts more effectively in $Adm^{hi/hi}$ mice than wildtype mice (Figure 5c). This lateralization phenotype observed in $Adm^{hi/hi}$ mice suggests increased gap junction function as intracellular Cx43 is targeted for degradation in injured cells.

We also found that we could reproduce this lateralization phenotype in cultured embryonic rat atrial cardiomyoblasts (H9c2) cells when treated with AM (Online Figure III). The cells also displayed prominent sub-cellular lateralization of Cx43, which could be nearly completely abrogated with the treatment of rAM24–50, a competitive inhibitor of AM.

Comparative expression of connexin proteins within the cardiac lymphatic vasculature in mice and humans.

Given the ability of AM to regulate Cx43 both *in vivo* and *in vitro* in both the myocardium and LECs, we sought to explicitly characterize the expression profile of connexins specifically within the cardiac lymphatic vasculature. Using paraffin sections of human heart tissue obtained from LVAD (left ventricular assist device) implantation surgery, we confirmed that human heart tissue expresses the same connexin proteins as the murine heart (Online Figure IV). Murine paraffin sections were obtained from male hearts after MI. Expression of connexins was evaluated by co-localization with Podoplanin, a marker of lymphatic vasculature. Cx43 and Cx47 were both expressed in cardiac lymphatics as evidenced by co-localization of Podoplanin in both humans and mouse, while Cx37 was entirely absent from the heart in both mouse and human (Online Figure IV). We further evaluated connexin protein expression in murine hearts by testing uninjured cardiac sections and evaluated staining in both $Adm^{hi/hi}$ and $Adm^{+/+}$ mice and saw no differences between genotype, nor did expression profile change after MI (data not shown). Overall, human and murine cardiac lymphatics appeared very similar in both morphology and density, while also expressing the same connexins.

AM and verapamil can linearize Cx43 and improve gap junction coupling within cultured human lymphatic endothelial (hLECs) cells.

To assess the effect that AM and Verapamil have on the function of gap junctions, we performed scrape loading assays, which permits the gap junction permeable dye, Lucifer Yellow, to travel through a cultured monolayer of hLECs after disrupting the monolayer by scraping a needle across the cells. We than visualize and quantify the passage of the dye through the cells in different conditions. As previously published, treatment of hLECs with AM increased gap junction formation, while pre-treatment with carbenoxolone (CBX), a gap junction inhibitor abrogated gap junction formation (Online Figure V)[39, 44]. Interestingly, verapamil, a drug used to treat hypertension and arrhythmias through targeting voltage-gated calcium channels, has recently been shown to have beneficial cardiovascular effects by preserving Cx43 expression [45]. Treatment of hLECs with verapamil had a very similar effect to AM and showed significant increase in gap junction formation (Figure 4a,b). To further

show that these gap junction coupling phenotypes were a direct result of Cx43 preservation at the cell membrane, we treated hLECs with both AM and verapamil and stained directly for Cx43 (Figure 4c). Both treatments resulted in very similar phenotypes, in which Cx43 localizes to the cell-membrane at cell-cell contacts, similar to the lateralization phenotypes we see *in vivo*. This phenomenon was lost when cells were pre-treated with CBX to inhibit gap junction formation.

Lymphatic-specific deletion of Cx43 results in defective permeability and function of lymphatic vasculature that cannot be rescued with AM treatment.

To further test the effect of Cx43 on lymphatic function, we generated a lymphatic-specific deletion of Cx43 using inducible Vegfr3-CreER (T2). To test the effects of Cx43 on permeability of lymphatic vessels, we used Evan's Blue Dye which can penetrate dermal lymphatics. Injection of 0.5% Evan's Blue intradermally in the ear showed rapid uptake in ear dermal lymphatics in *Vegfr3-CreER^{T2}; Cx43$^{fl/fl}$* and control mice (Figure 6a). However, after 5 minutes diffusion of the dye was largely exacerbated in *Vegfr3-CreER^{T2}; Cx43$^{fl/fl}$* mice compared to control mice. After 15 minutes, the diffusion of the dye persisted significantly in the *Vegfr3-CreER^{T2}; Cx43$^{fl/fl}$* mice.

We further tested permeability and function of dermal tail lymphatic vasculature by assessing *in vivo* lymphatic tail flow using fluorescent tail microlymphography in adult mice. Briefly, FITC-Dextran, a fluorescent dye, was injected directly into the interstitial space of the tail in the presence or absence of AM in *Vegfr3-CreER^{T2}; Cx43$^{fl/fl}$* and control mice. The ability of the dye to enter and flow through lymphatic capillaries was monitored over time. *Vegfr3-CreER^{T2}; Cx43$^{fl/fl}$* mice have lymphatic velocities nearly double that of control mice (Figure 6b). Consistent with previously published data, control mice had a slight but significant decrease in lymphatic velocity when co-injected with AM[13] (Figure 6b). However, in mice lacking Cx43, AM had no effect on lymphatic tail velocity. As summarized in Online Table I, individual lymphatic tail vasculature vessels were analyzed for morphology changes and changes in intensity of dye over time. Although morphology remained unchanged between genotypes or treatment groups over time (6–7 min post injection), control mice had a reduction in dye intensity (at 3 min and 6 min post injection) with AM treatment suggesting a reduction in dye volume within the individual lymphatic capillaries, consistent with the reduction in velocity. *Vegfr3-CreER^{T2}; Cx43$^{fl/fl}$* mice had no such effects with AM treatment; morphology and dye intensity remained constant over time with treatment.

We know that AM stabilizes endothelial junctions in LECs[13, 40]. It has previously been published that Cx43 and ZO-1 are bound at cell-cell junctions in the heart[46]. We confirmed this interaction in a proximal ligation assay (PLA) in untreated hLECs, an assay that tests for protein-protein interactions based on proximity between the proteins (Figure 6c). In some physiological conditions, like MI, ZO-1 has a higher affinity for c-Src than Cx43[46]. This causes Cx43 to disassociate from the cell membrane, making the gap junction non-functional[46, 47]. We treated hLECs with AM and stained for both Cx43 and ZO-1 (Figure 6d). Cells treated with AM showed more continuous ZO-1 junctions and increased Cx43 at the cell-cell membrane contacts compared to vehicle treated cells. We propose a model in

which AM stabilizes the binding of Cx43 and ZO-1 and endothelial junctions in LECs (Figure 6e).

DISCUSSION

It has recently been established that cardiac lymphangiogenesis and lymphatic remodeling is a common response to myocardial injury and cardiac diseases, yet the exact mechanisms regulating this phenomenon remain to be completely understood[9–11]. These vessels are primarily responsible for regulating fluid transport and trafficking of immune cells to clear edema and resolve inflammation, especially after MI[5, 48]. To further complicate such an intricate process, sex differences are prevalent but often underrepresented in cardiovascular disease related research. Anatomy, hormones, physiology, and cell signaling of the heart and its vasculature differ significantly between males and females[49]. In this study, we show for the first time that cardiac lymphatics have innate differences between the sexes.

Finding effective endogenous factors that positively regulate the cardiovascular healing process through lymphangiogenesis has been challenging. For example, VEGF-C induced lymphangiogenesis alone may not be enough to repair the post-MI heart[10]. AM levels increase endogenously in response to cardiac injury and disease, including MI[50]. Exogenous AM treatment has frequently been shown to be cardioprotective, but the exact mechanisms regulating this process are very dependent on experimental conditions[51–53]. The $Adm^{hi/hi}$ mouse model allows us to study the effect of global, constitutive overexpression of *Adm* for the first time without confounding factors such as injection time, dose, or viral delivery methods. We show that overexpression of *Adm* is not only sufficient to drive a proliferative response in cardiac lymphatic vasculature in both males and females, but also improve cardiac function one to two weeks after MI while suppressing cardiac edema. Given that increases in cardiac edema as small as 2% can have profound effects on cardiac output, this could be an extremely valuable therapeutic discovery[54, 55]. Overall, echocardiogram results, histology, and quantification of cardiac lymphatic vessels indicate that $Adm^{hi/hi}$ mice retain less fluid and undergo less remodeling, which likely can be attributed to the difference in lymphatic vasculature, since infarct size remains unchanged.

Resolution of cardiac edema has previously been shown to be bi-modal with peak increases in water content happening 3 hours after MI and resolving by 24 hours and a second peak happening 7 days after MI[56]. These studies though valuable were done using only male animal models. Our studies reveal interesting differences in the timing of cardiac edema resolution between males and females. Although we see very similar cardiac lymphatic vasculature by 15 days after MI in both male and female mice, improvements in cardiac function (ejection fraction and fractional shortening) are seen a full 5 days sooner in female mice. We also see profound differences in the resolution of hindpaw edema between males and females; $Adm^{hi/hi}$ females show significant improvement 1 day post CFA injection, while $Adm^{hi/hi}$ males see no significant improvement for 6 days. This may be due to developmental differences in cardiac lymphatic vasculature or other factors, like estrogen. Pre-menopausal women are innately protected from cardiovascular disease and heart failure, likely in part due to estrogen[57]. *Adm* expression can be induced by estrogen and is likely

regulated via estrogen-induced miRNAs[43, 58]. Further studies are needed to fully characterize how sex differences impact the lymphangiogenic repair process.

Previous studies have established that the main source of AM driving cardiac proliferation during development originates from the epicardium[42, 59]. Re-activation of the epicardium is known to be involved in cardiac remodeling and scar formation after myocardial injury through secretion of paracrine factors[60]. Our results further emphasize the importance of the epicardium in cardiac healing and remodeling after injury, while highlighting a novel role in cardiac lymphatic regulation. Like previous studies we see the majority of *de novo* vessels forming in the peri-infarct zone near the epicardium or the "epicardial border zone[61]." This paracrine signaling results not only in more vessels in $Adm^{hi/hi}$ mice, but the vessels are larger and more dilated indicative of differences in function.

Previous studies have characterized the importance of Cx37, Cx47, and Cx43 as the main connexin proteins expressed in developing lymphatic tissue[62, 63]. Mutations in these genes lead to lymphatic disorders in both mice and humans[27, 28, 30–32]. GJIC is involved in proper contraction of lymph vessels through the spreading of polarization currents[64]. However, it remains unknown what connexin proteins are expressed in the lymphatic vasculature specifically within the heart. Recent work showed that lymphatic cells within the heart have a unique, heterogeneous genetic origin that likely differs from other lymphatic systems[9]. We show here that Cx47 and Cx43 are expressed in the cardiac lymphatic vasculature, while Cx37 is notably absent from the lymphatic vessels in the heart in both murine and human tissue, making mice an ideal model for these studies. Mouse models with inducible lymphatic-specific deletion of C43 emphasize the requirement of Cx43 not only in development but maintenance of lymphatic function and also strengthen our findings that AM targets Cx43. Further characterization of how connexins regulate these vessels would be incredibly beneficial to fully unlocking the potential of targeting cardiac lymphatics as a therapeutic avenue.

It is already known that AM does not seem to affect expression or localization of Cx37 or Cx47 *in vitro,* but has the ability to increase mRNA and protein levels of Cx43 in hLECs while improving gap junction coupling function [39]. In our study, the increase in AM correlates to an overall elevation of Cx43 but more interestingly specific localization within cardiac LECs with preservation at the cell membrane. The previously characterized lateralization phenotype we see is associated with increased survival, increased cardiac conduction, and Cx43 stability[65–67]. During ischemia in the heart, the deprivation of oxygen within the cell lowers the pH and causes Cx43 to be targeted for degradation leading to consequences including arrhythmia[46, 47]. The role of Cx43 in electrical conduction of the heart is well established, and the lateralization of Cx43 is likely contributing to the increase in cardiac contractile function in border and remote zones, having a synergistic effect on the function of lymphatic vessels, which rely on cardiac contractions for effective lymph flow.

Verapamil is a drug that has been used to treat hypertension and arrhythmias through direct targeting of L-type Calcium channels[68]. However, it has also been shown to have indirect effects on the localization and stabilization of Cx43. By inhibiting calcium influx and preserving oxygen levels in the heart with verapamil, Cx43 is stabilized during injury

resulting in beneficial anti-arrhythmic phenotypes[45]. We used hLECs to show that verapamil has a similarly positive effect on the lateralization of Cx43 in lymphatics as it does in cardiomyocytes. Verapamil also had a positive effect on gap junction coupling *in vitro*. This discovery is a previously uncharacterized benefit of verapamil therapy for cardiac lymphatic function. AM was just as effective at gap junction coupling as verapamil in hLECs. As a protein that signals through a G-protein coupled receptor (GPCR), calcitonin receptor-like receptor (protein=CLR; gene=*Calcrl*) with specific co-receptor receptor-activity modifying protein 2 (RAMP2), adrenomedullin is an ideal candidate for a druggable biological target[69].

In conclusion, our data shows an endogenous lymphangiogenic response that is augmented by overexpression of *Adm*. We show that AM and verapamil can target Cx43 to increase gap junction coupling between hLECs. Our work highlights previously uncharacterized pathways and sex differences involved in cardiac lymphangiogenesis that preserve cardiac function and reduce edema. Further exploration of these and other factors could have profoundly beneficial effects in patients suffering from MI or other cardiovascular ailments.

Supplementary Material

Refer to Web version on PubMed Central for supplementary material.

ACKNOWLEDGEMENTS

We thank the University of North Carolina Animal Models Core, the University of North Carolina MHI Animal Surgery Core Lab, the University of North Carolina Histology Research Core, the University of North Carolina CGIBD Histology core, the University of North Carolina Hooker Imaging Core, and the University of North Carolina Microscopy Services Laboratory. We thank Dr. Sagrario Ortega for the use of the Vegfr3-CreER (T2) mice. We also thank Dr. James Faber, Dr. Pablo Ariel, Dr. Daniel Kechele, and members of the Caron laboratory for technical support and discussions.

SOURCES OF FUNDING

This work was supported by National Institutes of Health (NIH) grants HL129086 to K.M. Caron and an American Heart Association (AHA) Innovator Award 161RG27260077 to K.M. Caron, pre-doctoral grant 15PRE25680001 to C.E. Trincot, and Swiss National science Foundation grant 31ER30–160674 to T.V. Petrova. The Microscopy Services Laboratory, Department of Pathology and Laboratory Medicine, is supported in part by P30 CA016086 Cancer Center Core Support Grant to the UNC Lineberger Comprehensive Cancer Center. Research reported in this publication was supported in part by the North Carolina Biotech Center Institutional Support Grant 2016-IDG-1016.

Nonstandard Abbreviations and Acronyms:

***Adm*=gene**	AM=protein; adrenomedullin
Adm$^{hi/hi}$	adrenomedullin overexpression mouse
gene=*Calcrl*	calcitonin receptor-like receptor; protein=CLR
CBX	carbenoxolone
CFA	complete freund’s adjuvant
Cx43	connexin 43
hLECs	dermal human lymphatic endothelial cells

H9c2s	embryonic rat atrial cardiomyoblasts
GJIC	gap junction intercellular communication
GPCR	G-protein coupled receptor
LAD	left anterior descending
LECs	lymphatic endothelial cells
MR-proAM	mid-regional pro-adrenomedullin
MI	myocardial infarction
PLA	proximal ligation assay
RAMP2	receptor-activity modifying protein 2
Veh	vehicle
Verp	verapamil
WGA	wheat germ agglutinin

REFERENCES

1. Alitalo K The lymphatic vasculature in disease. Nat Med. 2011;17:1371–80.10.1038/nm.2545I. [PubMed: 22064427]
2. Schulte-Merker S, Sabine A and Petrova TV. Lymphatic vascular morphogenesis in development, physiology, and disease. J Cell Biol. 2011;193:607–18.10.1083/jcb.201012094I. [PubMed: 21576390]
3. Bradham RR, Parker EF, Barrington BA, Jr, Webb CM and Stallworth JM. The cardiac lymphatics. Ann Surg. 1970;171:899–902. [PubMed: 5420932]
4. Aspelund A, Robciuc MR, Karaman S, Makinen T and Alitalo K. Lymphatic System in Cardiovascular Medicine. Circulation research. 2016;118:515–30.10.1161/CIRCRESAHA.115.306544I. [PubMed: 26846644]
5. Vieira JM, Norman S, Villa Del Campo C, Cahill TJ, Barnette DN, Gunadasa-Rohling M, Johnson LA, Greaves DR, Carr CA, Jackson DG and Riley PR. The cardiac lymphatic system stimulates resolution of inflammation following myocardial infarction. The Journal of clinical investigation. 2018;10.1172/JCI97192I.
6. Davis KL, Laine GA, Geissler HJ, Mehlhorn U, Brennan M and Allen SJ. Effects of myocardial edema on the development of myocardial interstitial fibrosis. Microcirculation. 2000;7:269–80. [PubMed: 10963632]
7. Anand IS, Ferrari R, Kalra GS, Wahi PL, Poole-Wilson PA and Harris PC. Edema of cardiac origin. Studies of body water and sodium, renal function, hemodynamic indexes, and plasma hormones in untreated congestive cardiac failure. Circulation. 1989;80:299–305. [PubMed: 2752558]
8. Zia MI, Ghugre NR, Connelly KA, Strauss BH, Sparkes JD, Dick AJ and Wright GA. Characterizing myocardial edema and hemorrhage using quantitative T2 and T2* mapping at multiple time intervals post ST-segment elevation myocardial infarction. Circ Cardiovasc Imaging. 2012;5:566–72.10.1161/CIRCIMAGING.112.973222I. [PubMed: 22744938]
9. Klotz L, Norman S, Vieira JM, Masters M, Rohling M, Dube KN, Bollini S, Matsuzaki F, Carr CA and Riley PR. Cardiac lymphatics are heterogeneous in origin and respond to injury. Nature. 2015;522:62–7.10.1038/nature14483I. [PubMed: 25992544]
10. Henri O, Pouehe C, Houssari M, Galas L, Nicol L, Edwards-Levy F, Henry JP, Dumesnil A, Boukhalfa I, Banquet S, Schapman D, Thuillez C, Richard V, Mulder P and Brakenhielm E.

Selective Stimulation of Cardiac Lymphangiogenesis Reduces Myocardial Edema and Fibrosis Leading to Improved Cardiac Function Following Myocardial Infarction. Circulation. 2016;133:1484–97; discussion 1497.10.1161/CIRCULATIONAHA.115.020143I. [PubMed: 26933083]

11. Tatin F, Renaud-Gabardos E, Godet AC, Hantelys F, Pujol F, Morfoisse F, Calise D, Viars F, Valet P, Masri B, Prats AC and Garmy-Susini B. Apelin modulates pathological remodeling of lymphatic endothelium after myocardial infarction. JCI Insight. 2017;210.1172/jci.insight.93887I.
12. Caron KM and Smithies O. Extreme hydrops fetalis and cardiovascular abnormalities in mice lacking a functional Adrenomedullin gene. Proceedings of the National Academy of Sciences of the United States of America. 2001;98:615–9.10.1073/pnas.021548898I. [PubMed: 11149956]
13. Dunworth WP, Fritz-Six KL and Caron KM. Adrenomedullin stabilizes the lymphatic endothelial barrier in vitro and in vivo. Peptides. 2008;29:2243–9.10.1016/j.peptides.2008.09.009I. [PubMed: 18929609]
14. Kataoka Y, Miyazaki S, Yasuda S, Nagaya N, Noguchi T, Yamada N, Morii I, Kawamura A, Doi K, Miyatake K, Tomoike H and Kangawa K. The first clinical pilot study of intravenous adrenomedullin administration in patients with acute myocardial infarction. Journal of cardiovascular pharmacology. 2010;56:413–9.10.1097/FJC.0b013e3181f15b45I. [PubMed: 20930593]
15. Maisel A, Mueller C, Nowak R, Peacock WF, Landsberg JW, Ponikowski P, Mockel M, Hogan C, Wu AH, Richards M, Clopton P, Filippatos GS, Di Somma S, Anand I, Ng L, Daniels LB, Neath SX, Christenson R, Potocki M, McCord J, Terracciano G, Kremastinos D, Hartmann O, von Haehling S, Bergmann A, Morgenthaler NG and Anker SD. Mid-region pro-hormone markers for diagnosis and prognosis in acute dyspnea: results from the BACH (Biomarkers in Acute Heart Failure) trial. Journal of the American College of Cardiology. 2010;55:2062–76.10.1016/j.jacc.2010.02.025I. [PubMed: 20447528]
16. Morbach C, Marx A, Kaspar M, Guder G, Brenner S, Feldmann C, Stork S, Vollert JO, Ertl G, Angermann CE, Group INHS and the Competence Network Heart FPrognostic potential of midregional pro-adrenomedullin following decompensation for systolic heart failure: comparison with cardiac natriuretic peptides. Eur J Heart Fail. 2017;19:1166–1175.10.1002/ejhf.859I. [PubMed: 28516504]
17. Jougasaki M and Burnett JC, Jr, Adrenomedullin: potential in physiology and pathophysiology. Life sciences. 2000;66:855–72. [PubMed: 10714887]
18. Meens MJ, Kwak BR and Duffy HS. Role of connexins and pannexins in cardiovascular physiology. Cell Mol Life Sci. 2015;72:2779–92.10.1007/s00018-015-1959-2I. [PubMed: 26091747]
19. Sohl G and Willecke K. Gap junctions and the connexin protein family. Cardiovascular research. 2004;62:228–32.10.1016/j.cardiores.2003.11.013I. [PubMed: 15094343]
20. Unger VM, Kumar NM, Gilula NB and Yeager M. Three-dimensional structure of a recombinant gap junction membrane channel. Science. 1999;283:1176–80. [PubMed: 10024245]
21. Alexander DB and Goldberg GS. Transfer of biologically important molecules between cells through gap junction channels. Curr Med Chem. 2003;10:2045–58. [PubMed: 12871102]
22. Zong L, Zhu Y, Liang R and Zhao HB. Gap junction mediated miRNA intercellular transfer and gene regulation: A novel mechanism for intercellular genetic communication. Sci Rep. 2016;6:1988410.1038/srep19884I. [PubMed: 26814383]
23. Cherian PP, Cheng B, Gu S, Sprague E, Bonewald LF and Jiang JX. Effects of mechanical strain on the function of Gap junctions in osteocytes are mediated through the prostaglandin EP2 receptor. The Journal of biological chemistry. 2003;278:43146–56.10.1074/jbc.M302993200I. [PubMed: 12939279]
24. Ongstad EL, O'Quinn MP, Ghatnekar GS, Yost MJ and Gourdie RG. A Connexin43 Mimetic Peptide Promotes Regenerative Healing and Improves Mechanical Properties in Skin and Heart. Advances in wound care. 2013;2:55–62.10.1089/wound.2011.0341I. [PubMed: 24527326]
25. Roell W, Lewalter T, Sasse P, Tallini YN, Choi BR, Breitbach M, Doran R, Becher UM, Hwang SM, Bostani T, von Maltzahn J, Hofmann A, Reining S, Eiberger B, Gabris B, Pfeifer A, Welz A, Willecke K, Salama G, Schrickel JW, Kotlikoff MI and Fleischmann BK. Engraftment of connexin

43-expressing cells prevents post-infarct arrhythmia. Nature. 2007;450:819–24.10.1038/nature06321I. [PubMed: 18064002]

26. Fernandes S, van Rijen HV, Forest V, Evain S, Leblond AL, Merot J, Charpentier F, de Bakker JM and Lemarchand P. Cardiac cell therapy: overexpression of connexin43 in skeletal myoblasts and prevention of ventricular arrhythmias. J Cell Mol Med. 2009;13:3703–12.10.1111/j.1582-4934.2009.00740.xI. [PubMed: 19438811]
27. Kanady JD, Dellinger MT, Munger SJ, Witte MH and Simon AM. Connexin37 and Connexin43 deficiencies in mice disrupt lymphatic valve development and result in lymphatic disorders including lymphedema and chylothorax. Developmental biology. 2011;354:253–66.10.1016/j.ydbio.2011.04.004I. [PubMed: 21515254]
28. Munger SJ, Davis MJ and Simon AM. Defective lymphatic valve development and chylothorax in mice with a lymphatic-specific deletion of Connexin43. Developmental biology. 2017;421:204–218.10.1016/j.ydbio.2016.11.017I. [PubMed: 27899284]
29. Glass AM, Snyder EG and Taffet SM. Connexins and pannexins in the immune system and lymphatic organs. Cell Mol Life Sci. 2015;72:2899–910.10.1007/s00018-015-1966-3I. [PubMed: 26100515]
30. Brice G, Ostergaard P, Jeffery S, Gordon K, Mortimer PS and Mansour S. A novel mutation in GJA1 causing oculodentodigital syndrome and primary lymphoedema in a three generation family. Clin Genet. 2013;84:378–81.10.1111/cge.12158I. [PubMed: 23550541]
31. Ferrell RE, Baty CJ, Kimak MA, Karlsson JM, Lawrence EC, Franke-Snyder M, Meriney SD, Feingold E and Finegold DN. GJC2 missense mutations cause human lymphedema. Am J Hum Genet. 2010;86:943–8.10.1016/j.ajhg.2010.04.010I. [PubMed: 20537300]
32. Finegold DN, Baty CJ, Knickelbein KZ, Perschke S, Noon SE, Campbell D, Karlsson JM, Huang D, Kimak MA, Lawrence EC, Feingold E, Meriney SD, Brufsky AM and Ferrell RE. Connexin 47 mutations increase risk for secondary lymphedema following breast cancer treatment. Clin Cancer Res. 2012;18:2382–90.10.1158/1078-0432.CCR-11-2303I. [PubMed: 22351697]
33. Li M, Schwerbrock NM, Lenhart PM, Fritz-Six KL, Kadmiel M, Christine KS, Kraus DM, Espenschied ST, Willcockson HH, Mack CP and Caron KM. Fetal-derived adrenomedullin mediates the innate immune milieu of the placenta. The Journal of clinical investigation. 2013;123:2408–20.10.1172/JCI67039I. [PubMed: 23635772]
34. Liao Y, Day KH, Damon DN and Duling BR. Endothelial cell-specific knockout of connexin 43 causes hypotension and bradycardia in mice. Proceedings of the National Academy of Sciences of the United States of America. 2001;98:9989–94.10.1073/pnas.171305298I. [PubMed: 11481448]
35. Martinez-Corral I, Stanczuk L, Frye M, Ulvmar MH, Dieguez-Hurtado R, Olmeda D, Makinen T and Ortega S. Vegfr3-CreER (T2) mouse, a new genetic tool for targeting the lymphatic system. Angiogenesis. 2016;19:433–45.10.1007/s10456-016-9505-xI. [PubMed: 26993803]
36. Renier N, Wu Z, Simon DJ, Yang J, Ariel P and Tessier-Lavigne M. iDISCO: a simple, rapid method to immunolabel large tissue samples for volume imaging. Cell. 2014;159:896–910.10.1016/j.cell.2014.10.010I. [PubMed: 25417164]
37. Kechele DO, Dunworth WP, Trincot CE, Wetzel-Strong SE, Li M, Ma H, Liu J and Caron KM. Endothelial Restoration of Receptor Activity-Modifying Protein 2 Is Sufficient to Rescue Lethality, but Survivors Develop Dilated Cardiomyopathy. Hypertension. 2016;68:667–77.10.1161/HYPERTENSIONAHA.116.07191I. [PubMed: 27402918]
38. Takagawa J, Zhang Y, Wong ML, Sievers RE, Kapasi NK, Wang Y, Yeghiazarians Y, Lee RJ, Grossman W and Springer ML. Myocardial infarct size measurement in the mouse chronic infarction model: comparison of area- and length-based approaches. J Appl Physiol (1985). 2007;102:2104–11.10.1152/japplphysiol.00033.2007I. [PubMed: 17347379]
39. Karpinich NO and Caron KM. Gap junction coupling is required for tumor cell migration through lymphatic endothelium. Arterioscler Thromb Vasc Biol. 2015;35:1147–55.10.1161/ATVBAHA.114.304752I. [PubMed: 25792452]
40. Hoopes SL, Willcockson HH and Caron KM. Characteristics of multi-organ lymphangiectasia resulting from temporal deletion of calcitonin receptor-like receptor in adult mice. PloS one. 2012;7:e4526110.1371/journal.pone.0045261I. [PubMed: 23028890]

41. Ratajska A, Gula G, Flaht-Zabost A, Czarnowska E, Ciszek B, Jankowska-Steifer E, Niderla-Bielinska J and Radomska-Lesniewska D. Comparative and developmental anatomy of cardiac lymphatics. ScientificWorldJournal. 2014;2014:18317010.1155/2014/183170I. [PubMed: 24592145]

42. Wetzel-Strong SE, Li M, Klein KR, Nishikimi T and Caron KM. Epicardial-derived adrenomedullin drives cardiac hyperplasia during embryogenesis. Developmental Dynamics. 2014;243:243–256. [PubMed: 24123312]

43. Sarah E Wetzel-Strong ML, Espenschied Scott T., Caron Kathleen M.. Estrogen-induced microRNAs balance adrenomedullin expression. American Journal of Physiology Regulatory, Integrative, and Comparitive Physiology. 2015;

44. Goldberg GS, Moreno AP, Bechberger JF, Hearn SS, Shivers RR, MacPhee DJ, Zhang YC and Naus CC. Evidence that disruption of connexon particle arrangements in gap junction plaques is associated with inhibition of gap junctional communication by a glycyrrhetinic acid derivative. Exp Cell Res. 1996;222:48–53.10.1006/excr.1996.0006I. [PubMed: 8549672]

45. Zhou P, Zhang SM, Wang QL, Wu Q, Chen M and Pei JM. Anti-arrhythmic effect of verapamil is accompanied by preservation of cx43 protein in rat heart. PloS one. 2013;8:e7156710.1371/journal.pone.0071567I. [PubMed: 23951191]

46. Kieken F, Mutsaers N, Dolmatova E, Virgil K, Wit AL, Kellezi A, Hirst-Jensen BJ, Duffy HS and Sorgen PL. Structural and molecular mechanisms of gap junction remodeling in epicardial border zone myocytes following myocardial infarction. Circulation research. 2009;104:1103–12.10.1161/CIRCRESAHA.108.190454I. [PubMed: 19342602]

47. Matsushita T, Oyamada M, Fujimoto K, Yasuda Y, Masuda S, Wada Y, Oka T and Takamatsu T. Remodeling of cell-cell and cell-extracellular matrix interactions at the border zone of rat myocardial infarcts. Circulation research. 1999;85:1046–55. [PubMed: 10571536]

48. Cahill TJ, Choudhury RP and Riley PR. Heart regeneration and repair after myocardial infarction: translational opportunities for novel therapeutics. Nat Rev Drug Discov. 2017;10.1038/nrd.2017.106I.

49. Boese AC, Kim SC, Yin KJ, Lee JP and Hamblin MH. Sex differences in vascular physiology and pathophysiology: estrogen and androgen signaling in health and disease. American journal of physiology Heart and circulatory physiology. 2017;313:H524–H545.10.1152/ajpheart.00217.2016I. [PubMed: 28626075]

50. Gibbons C, Dackor R, Dunworth W, Fritz-Six K and Caron KM. Receptor activity-modifying proteins: RAMPing up adrenomedullin signaling. Molecular endocrinology. 2007;21:783–96.10.1210/me.2006-0156I. [PubMed: 17053041]

51. Hamid SA, Totzeck M, Drexhage C, Thompson I, Fowkes RC, Rassaf T and Baxter GF. Nitric oxide/cGMP signalling mediates the cardioprotective action of adrenomedullin in reperfused myocardium. Basic research in cardiology. 2010;105:257–66.10.1007/s00395-009-0058-7I. [PubMed: 19714395]

52. Kato K, Yin H, Agata J, Yoshida H, Chao L and Chao J. Adrenomedullin gene delivery attenuates myocardial infarction and apoptosis after ischemia and reperfusion. American journal of physiology Heart and circulatory physiology. 2003;285:H1506–14.10.1152/ajpheart.00270.2003I. [PubMed: 12805025]

53. Wei X, Zhao C, Jiang J, Li J, Xiao X and Wang DW. Adrenomedullin gene delivery alleviates hypertension and its secondary injuries of cardiovascular system. Human gene therapy. 2005;16:372–80.10.1089/hum.2005.16.372I. [PubMed: 15812232]

54. Laine GA and Allen SJ. Left ventricular myocardial edema. Lymph flow, interstitial fibrosis, and cardiac function. Circulation research. 1991;68:1713–21. [PubMed: 2036720]

55. Dongaonkar RM, Stewart RH, Geissler HJ and Laine GA. Myocardial microvascular permeability, interstitial oedema, and compromised cardiac function. Cardiovascular research. 2010;87:331–9.10.1093/cvr/cvq145I. [PubMed: 20472566]

56. Fernandez-Jimenez R, Sanchez-Gonzalez J, Aguero J, Garcia-Prieto J, Lopez-Martin GJ, Garcia-Ruiz JM, Molina-Iracheta A, Rossello X, Fernandez-Friera L, Pizarro G, Garcia-Alvarez A, Dall'Armellina E, Macaya C, Choudhury RP, Fuster V and Ibanez B. Myocardial edema after ischemia/reperfusion is not stable and follows a bimodal pattern: imaging and histological tissue

characterization. Journal of the American College of Cardiology. 2015;65:315–323.10.1016/j.jacc.2014.11.004I. [PubMed: 25460833]

57. Moolman JA. Unravelling the cardioprotective mechanism of action of estrogens. Cardiovascular research. 2006;69:777–80. [PubMed: 16532550]
58. Watanabe H, Takahashi E, Kobayashi M, Goto M, Krust A, Chambon P and Iguchi T. The estrogen-responsive adrenomedullin and receptor-modifying protein 3 gene identified by DNA microarray analysis are directly regulated by estrogen receptor. Journal of molecular endocrinology. 2006;36:81–9.10.1677/jme.1.01825I. [PubMed: 16461929]
59. Klein KR, Karpinich NO, Espenschied ST, Willcockson HH, Dunworth WP, Hoopes SL, Kushner EJ, Bautch VL and Caron KM. Decoy receptor CXCR7 modulates adrenomedullin-mediated cardiac and lymphatic vascular development. Dev Cell. 2014;30:528–40.10.1016/j.devcel.2014.07.012I. [PubMed: 25203207]
60. Zhou B, Honor LB, He H, Ma Q, Oh JH, Butterfield C, Lin RZ, Melero-Martin JM, Dolmatova E, Duffy HS, Gise A, Zhou P, Hu YW, Wang G, Zhang B, Wang L, Hall JL, Moses MA, McGowan FX and Pu WT. Adult mouse epicardium modulates myocardial injury by secreting paracrine factors. The Journal of clinical investigation. 2011;121:1894–904.10.1172/JCI45529I. [PubMed: 21505261]
61. Sun QN, Wang YF and Guo ZK. Reconstitution of myocardial lymphatic vessels after acute infarction of rat heart. Lymphology. 2012;45:80–6. [PubMed: 23057153]
62. Munger SJ, Geng X, Srinivasan RS, Witte MH, Paul DL and Simon AM. Segregated Foxc2, NFATc1 and Connexin expression at normal developing venous valves, and Connexin-specific differences in the valve phenotypes of Cx37, Cx43, and Cx47 knockout mice. Developmental biology. 2016;412:173–90.10.1016/j.ydbio.2016.02.033I. [PubMed: 26953188]
63. Sabine A, Agalarov Y, Maby-El Hajjami H, Jaquet M, Hagerling R, Pollmann C, Bebber D, Pfenniger A, Miura N, Dormond O, Calmes JM, Adams RH, Makinen T, Kiefer F, Kwak BR and Petrova TV. Mechanotransduction, PROX1, and FOXC2 cooperate to control connexin37 and calcineurin during lymphatic-valve formation. Dev Cell. 2012;22:430–45.10.1016/j.devcel.2011.12.020I. [PubMed: 22306086]
64. Zawieja DC, Davis KL, Schuster R, Hinds WM and Granger HJ. Distribution, propagation, and coordination of contractile activity in lymphatics. Am J Physiol. 1993;264:H1283–91. [PubMed: 8476104]
65. Qu J, Volpicelli FM, Garcia LI, Sandeep N, Zhang J, Marquez-Rosado L, Lampe PD and Fishman GI. Gap junction remodeling and spironolactone-dependent reverse remodeling in the hypertrophied heart. Circulation research. 2009;104:365–71.10.1161/CIRCRESAHA.108.184044I. [PubMed: 19096029]
66. Peters NS, Coromilas J, Severs NJ and Wit AL. Disturbed connexin43 gap junction distribution correlates with the location of reentrant circuits in the epicardial border zone of healing canine infarcts that cause ventricular tachycardia. Circulation. 1997;95:988–96. [PubMed: 9054762]
67. Chkourko HS, Guerrero-Serna G, Lin X, Darwish N, Pohlmann JR, Cook KE, Martens JR, Rothenberg E, Musa H and Delmar M. Remodeling of mechanical junctions and of microtubule-associated proteins accompany cardiac connexin43 lateralization. Heart Rhythm. 2012;9:1133–1140 e6.10.1016/j.hrthm.2012.03.003I. [PubMed: 22406144]
68. Curtis MJ and Walker MJ. The mechanism of action of the optical enantiomers of verapamil against ischaemia-induced arrhythmias in the conscious rat. Br J Pharmacol. 1986;89:137–47. [PubMed: 3801768]
69. McLatchie LM, Fraser NJ, Main MJ, Wise A, Brown J, Thompson N, Solari R, Lee MG and Foord SM. RAMPs regulate the transport and ligand specificity of the calcitonin-receptor-like receptor. Nature. 1998;393:333–9.10.1038/30666I. [PubMed: 9620797]

NOVELTY AND SIGNIFICANCE

What Is Known?

- Cardiac lymphatics proliferate in response to myocardial infarction (MI).
- Cardiac lymphatics may improve cardiac function and prevent the formation of scar tissue after MI.
- The cardioprotective peptide - adrenomedullin (AM) is expressed in lymphatic vessels.

What New Information Does This Article Contribute?

- Cardiac lymphatics differ between males and females.
- AM contributes to cardiac lymphangiogenesis post-MI.
- AM can regulate Cx43, which may be vital for the proper functioning of cardiac lymphatics.

Cardiac lymphatics are new, potential therapeutic targets, especially in the context of MI. Although it is known that cardiac disease and injury affect men and women differently, sex differences in cardiac lymphatics have not been studied. Here we show that cardiac lymphatics develop differently in males and females, but in both sexes, AM can augment growth of cardiac lymphatics after MI, which contributes to increased cardiac function and less cardiac edema. We also found that within cardiac lymphatics both mice and humans express the same connexin proteins and that Cx43, a protein regulated by AM, contributes to the function of these vessels.

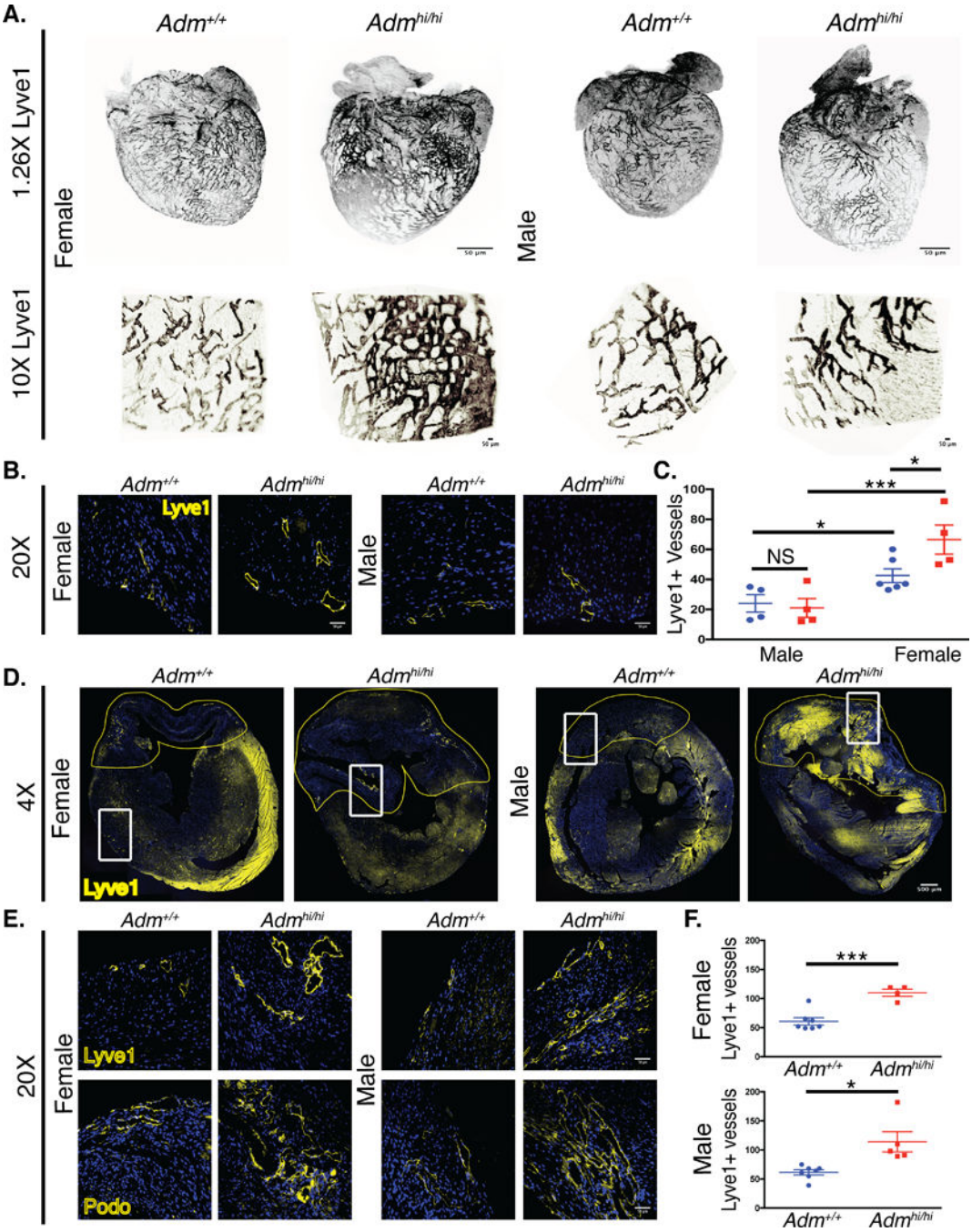

Figure 1: *Adm* drives sex-dependent cardiac lymphangiogenesis during development and surgical model of MI.

A. Light sheet 3-D microscopy for cardiac lymphatic vasculature in healthy adult male and female wild-type ($Adm^{+/+}$) and $Adm^{hi/hi}$ mice (black=Lyve1); scale bar= 50μm B. Immunohistochemistry of cardiac sections in healthy adult male and female $Adm^{+/+}$ and $Adm^{hi/hi}$ mice (yellow=Lyve1, blue=DAPI); scale bar=50μm C. Lyve1+ vessels/section in adult male mice (n=4 for all groups) and adult female mice (n=6 $Adm^{+/+}$; n=4 $Adm^{hi/hi}$) NS P>0.05, *P<0.05, ***P<0.001 by Uncorrected Fisher's LSD 2way ANOVA. D. Immunohistochemistry of cardiac sections in infarcted adult $Adm^{+/+}$ and $Adm^{hi/hi}$ mice 15–

21 days (d) post-MI (yellow=Lyve1, blue=DAPI); scale bar= 500μm, 50μm. Infarct zone is outlined and boxed zone is highlighted in panels below (E). E. (yellow=Lyve1, Podoplanin; blue=DAPI); scale bar=50μm F. Quantification of Lyve1+ vessels 15–21 d post-MI (n=7 $Adm^{+/+}$; 4–5 $Adm^{hi/hi}$) * P<0.05, ***P<0.001 by unpaired student's two-tailed *t* test with Welch's correction. Mean ±SEM is shown.

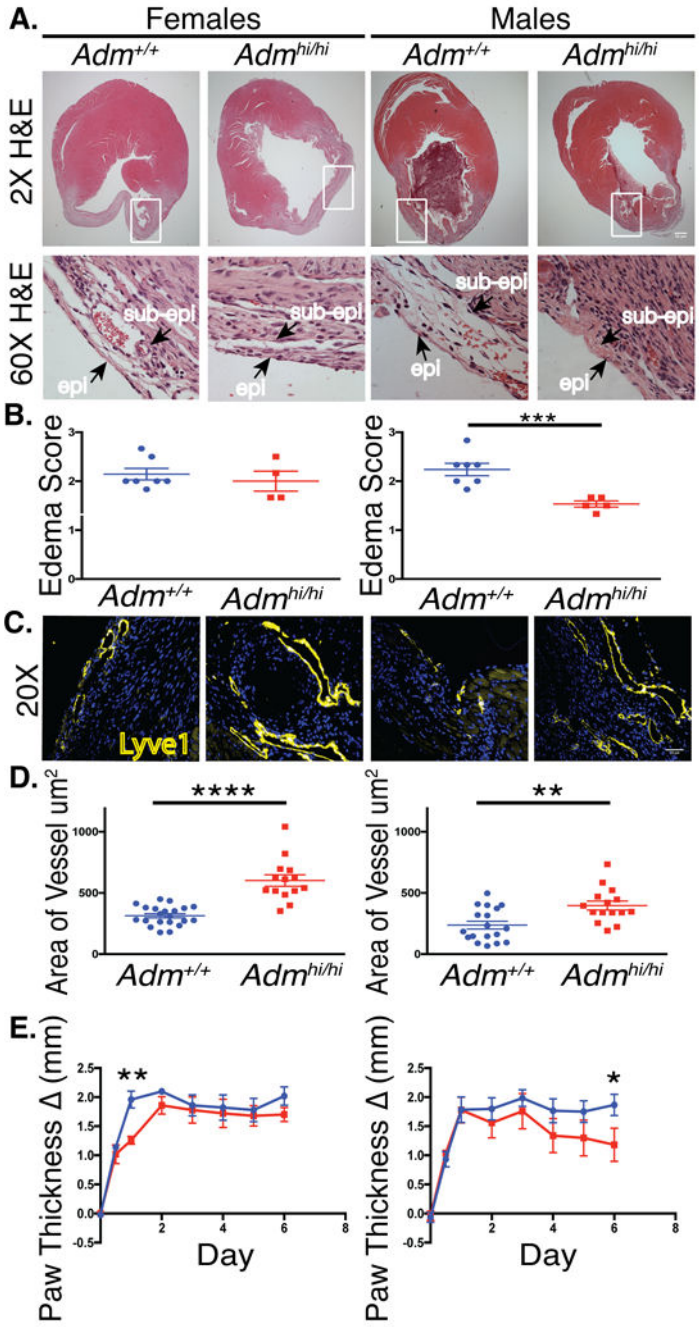

Figure 2: Overexpression of *Adm* results in less edema and dilated cardiac lymphatic vasculature post-MI.

A. Histology hematoxylin-eosin (H&E) of cardiac sections 15–21 d post-MI with infarcted boxed area highlighted in panels below, with epicardial (epi) and sub-epicardial (sub-epi) layers highlighted with arrows; scale bar=50μm, 1000μm B. Quantification of edema 15–21 d post-MI (n=7 $Adm^{+/+}$; 4–5 $Adm^{hi/hi}$) ***P<0.001 by unpaired student's two-tailed *t* test with Welch's correction. Mean ±SEM is shown. Statistical significance (P=0.0013 in males; P>0.05 in females) is confirmed with nonparametric tests, Mann-Whitney and Kolmogorov-Smirnov. C. Immunohistochemistry of cardiac sections in infarcted adult $Adm^{+/+}$ and

$Adm^{hi/hi}$ mice 15–21 d post-MI (yellow=Lyve1, blue=DAPI;) scale bar= 50μm D. Quantification of vessel area (μm^2) 15–21 d post-MI (n=6–7 $Adm^{+/+}$; 5 $Adm^{hi/hi}$) **P<0.001, ****P<0.0001 by unpaired student's two-tailed *t* test with Welch's correction. Mean ±SEM is shown. E. Quantification of paw thickness normalized to uninjected paw (mm) (n=5–6 $Adm^{+/+}$; 4–5 $Adm^{hi/hi}$) *P<0.05 by unpaired student's two-tailed *t* test with Welch's correction. Mean ±SEM is shown.

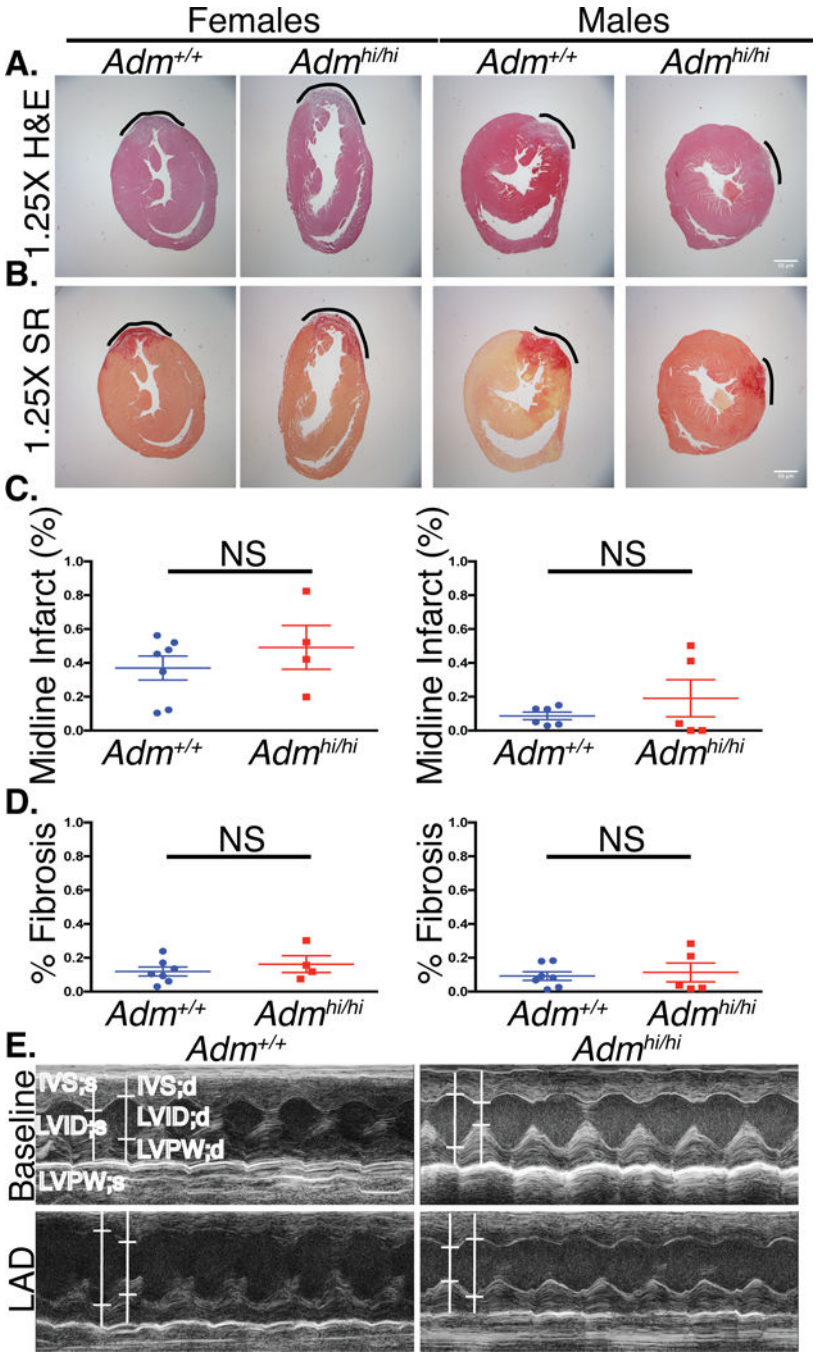

Figure 3: Overexpression of *Adm* correlates with improved cardiac function post-MI.

A. Histology hematoxylin-eosin (H&E) with infarcted area outlined & B. Fibrosis Picrosirius Red (SR) of cardiac sections 15–21 d post-MI with fibrotic area outlined; scale bar=50μm. C. Quantification of infarct size & D. Fibrotic area 15–21 d post-MI (n=7 $Adm^{+/+}$; 4–5 $Adm^{hi/hi}$) NS P>0.05, by unpaired student's two-tailed *t* test with Welch's correction. Mean ±SEM is shown. E. Representative M-mode echocardiograms from left ventricles of $Adm^{+/+}$ and $Adm^{hi/hi}$ male mice before and after (15 days) MI with echo measurements labeled.

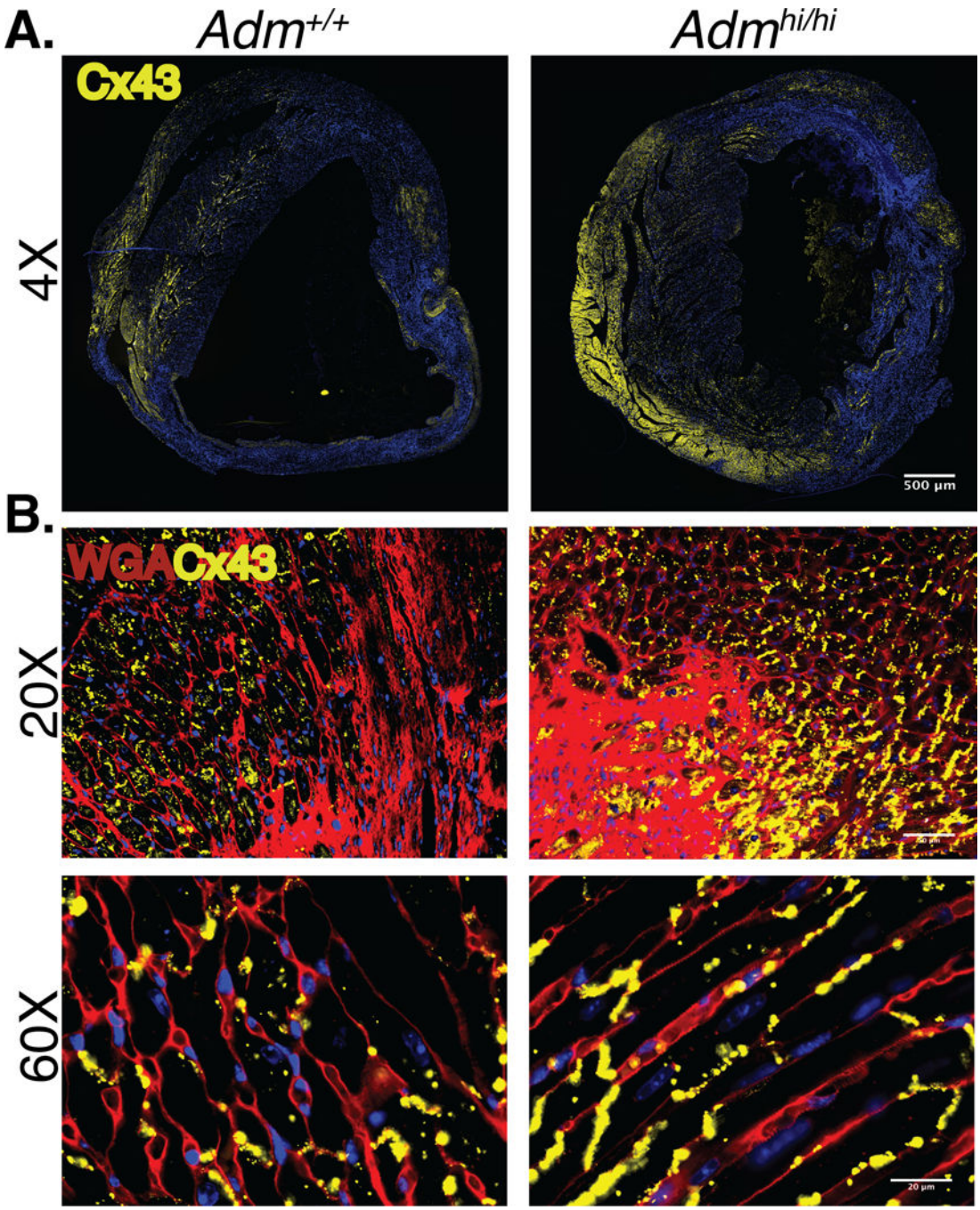

Figure 4: Adrenomedullin affects localization of Cx43 in injured myocardium.

A. Immunohistochemistry of cardiac sections in infarcted adult male *Adm*$^{+/+}$ and *Adm*$^{hi/hi}$ 10–15 d post-MI (yellow=Cx43, blue=DAPI); scale bar=500µm. B. Immunohistochemistry of cardiac sections in peri-infarct zone of adult male *Adm*$^{+/+}$ and *Adm*$^{hi/hi}$ mice 10–15 d post-MI (yellow=Cx43, red=WGA, blue=DAPI); scale bar=50µm, 20µm.

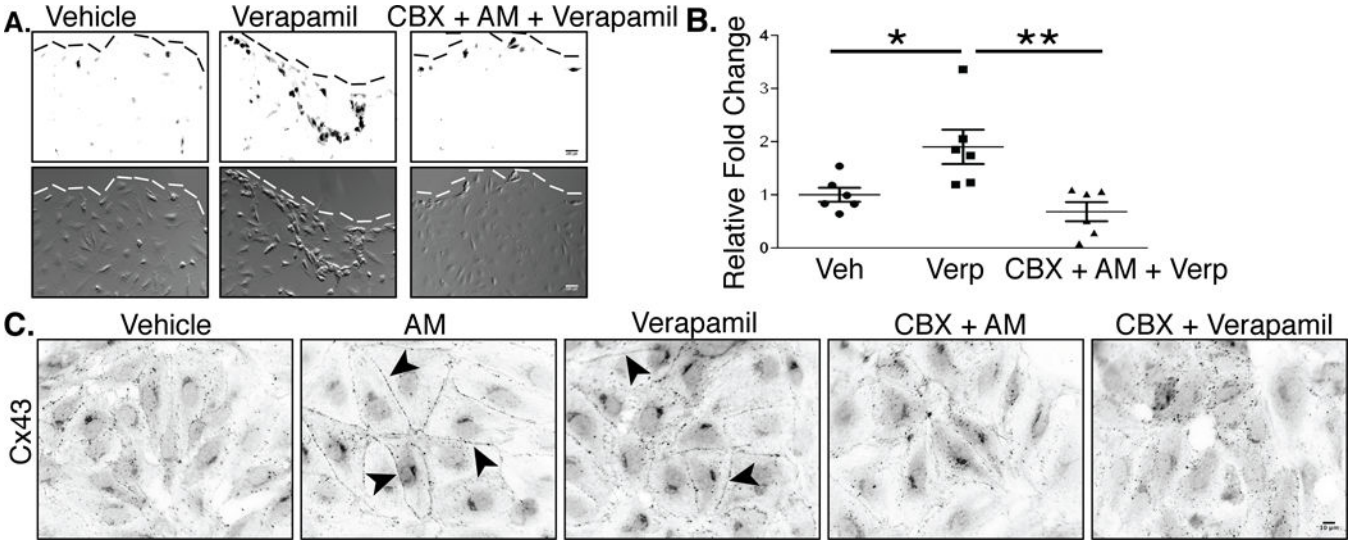

Figure 5: AM and verapamil can linearize Cx43 and improve gap junction coupling within cultured human lymphatic endothelial (hLECs) cells.

A. Transfer of Lucifer yellow dye through hLECs was imaged after scrape loading. Cells were pre-treated with gap junction inhibitor CBX (100μM) for 30 minutes followed by treatment with verapamil (10μM) for 15 minutes; scale bar=50μm. B. The percentage of dye coupled cells was quantified by dividing the number of Lucifer yellow-positive cells by the total number of cells in the field using Image J threshold. *P<0.05, **P<0.01 by Tukey's Multiple comparisons test 1way ANOVA. Mean ±SEM is shown. C. Cx43 expression and localization in response to AM and verapamil treatment. hLECs were pretreated with CBX (100μM) for 30 minutes followed by treatment with hAM (10nM) or verapamil (10μM) for 15 minutes and stained for Cx43. Arrows highlight Cx43 at cell-cell contacts; scale bar=10μm.

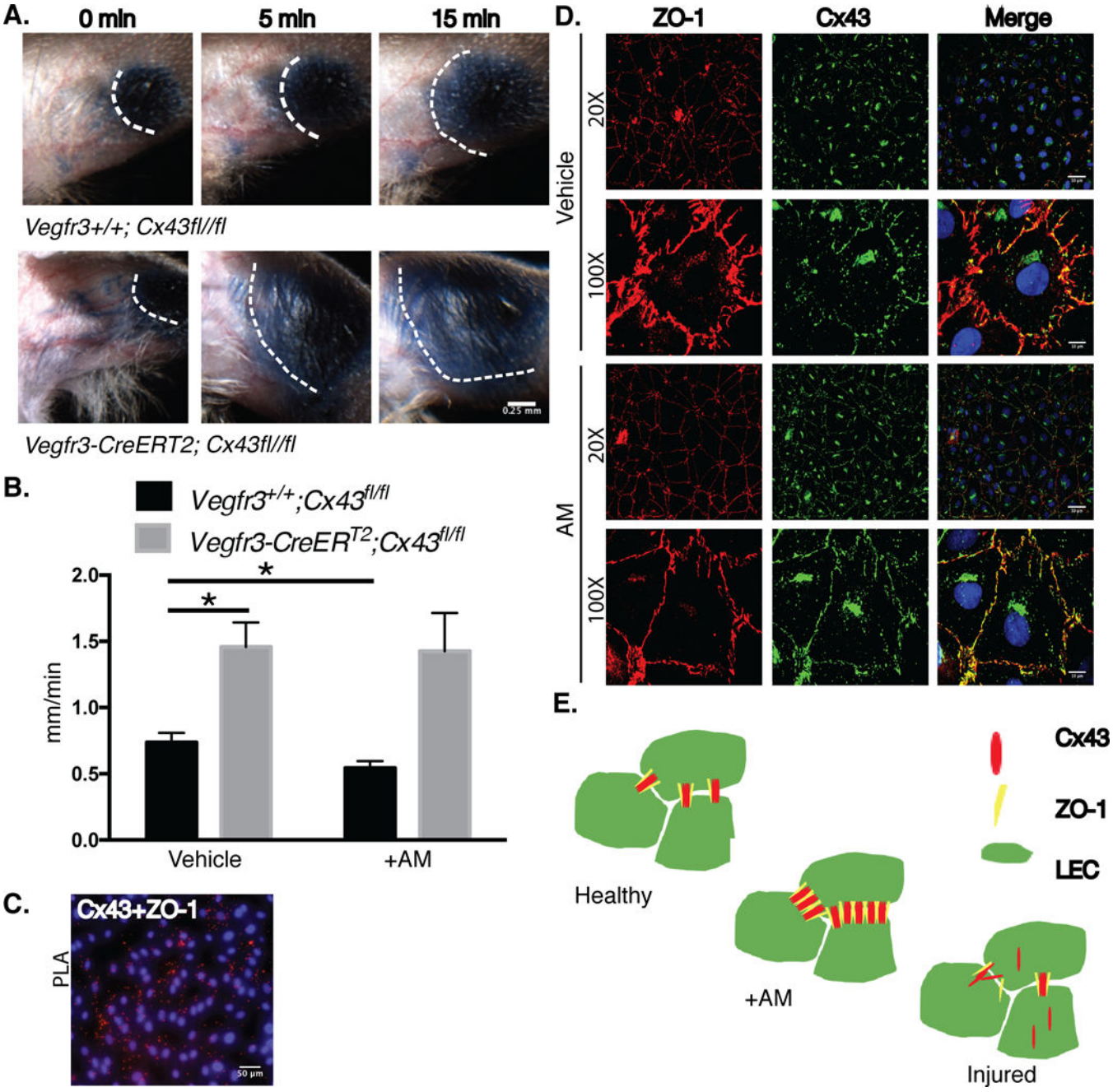

Figure 6: Lymphatic-specific Cx43 deletion leads to defective lymphatic vessels; AM targets Cx43 to tighten and linearize junctions in LECs.

A. *In vivo* lymphatic permeability assay assessing the leakage of Evan's blue dye from the dermal lymphatic vessels in the ear. Images represent Evan's blue dye location directly after the injection of the dye, 5 minutes, and 15 minutes post injection; scale bar=0.25mm. B. *In vivo* tail microlymphography assessed velocity of dye transport in tail lymphatics with and without AM co-injection. *P<0.05 by unpaired student's two-tailed *t* test with Welch's correction. Mean ±SEM is shown. C. PLA Cx43 and ZO-1 interaction in hLECs; scale bar=50µm. D. Cx43 and ZO-1 expression and localization in response to hAM (10nM)

treatment for 15 minutes; scale bar=50μm, 10μm. E. AM increases Cx43 and ZO-1 interactions in hLECs.

Table 1:

Echocardiogram analysis of $Adm^{+/+}$ and $Adm^{hi/hi}$ males before and after MI. BPM indicates beats per minutes; CO, cardiac output; d, diastolic; EF, ejection fraction; FS, fractional shortening; IVS, interventricular septal; LV, left ventricle; LVID, left ventricle internal diameter; LVPW, left ventricle posterior wall; and s, systole.

	Baseline		5 Days Post LAD		10 Days Post LAD		15 Days Post LAD	
	***Adm*$^{+/+}$**	***Adm*$^{hi/hi}$**	***Adm*$^{+/+}$**	***Adm*$^{hi/hi}$**	***Adm*$^{+/+}$**	***Adm*$^{hi/hi}$**	***Adm*$^{+/+}$**	***Adm*$^{hi/hi}$**
IVS;d mm	1.17±0.03	1.16±0.03	1.01±0.08	1.27 *±0.06	1.03±0.09	1.10±0.11	0.94±0.09	1.29 †±0.05
IVS;s mm	1.87±0.04	1.87±0.03	1.27±0.13	1.67 *±0.10	1.36±0.15	1.50±0.16	1.21±0.13	1.95 ‡±0.08
LVID;d mm	2.79±0.08	2.99±0.09	4.033±0.20	4.10±0.18	4.07±0.18	3.84±0.20	3.95±0.19	3.60±0.15
LVID;s mm	1.41±0.07	1.58±0.10	3.25±0.21	3.52±0.25	3.18±0.21	2.84±0.18	3.21±0.23	2.35 †±0.20
LVPW;d mm	1.01±0.03	1.13 *±0.05	1.21±0.09	1.05±0.05	1.19±0.07	1.08±0.06	1.32±0.09	1.27±0.14
LVPW;s mm	1.75±0.06	1.80±0.07	1.46±0.11	1.38±0.06	1.48±0.09	1.47±0.07	1.66±0.11	1.82±0.13
LV Mass mg	112.5±6.06	129.0±7.08	185.0±12.92	214.2±12.41	190.1±10.27	180.4±13.80	191.6±19.35	200.2±21.11
LV Mass (Corrected) mg	90.04±4.85	103.2±5.66	148.0±10.33	171.4±9.93	152.0±8.22	144.3±11.04	153.3±15.48	160.2±16.89
LV Vol;d µl	30.58±1.86	36.26±2.81	76.21±8.35	70.82±5.92	70.40±6.56	67.13±7.68	70.82±8.15	55.28±5.33
LV Vol;s µl	6.07±0.75	8.25±1.22	48.01±7.04	36.16±4.86	39.17±5.31	33.29±5.11	45.60±7.96	20.84 *±3.92
EF %	81.93±1.62	79.55±1.89	41.04±3.80	48.99±4.05	45.07±3.53	49.40±4.70	39.67±4.13	64.03 †±4.61
FS %	50.55±1.77	48.11±1.95	20.50±2.28	25.27±2.45	22.64±2.07	25.62±2.94	19.46±2.31	35.08 †±3.64
Heart Rate BPM	637.7±13.06	603.2±13.67	653.7±17.66	582.2 *±24.90	689.7±5.49	598.1 †±25.97	685.7±10.76	657.1±20.69
CO (Approx.) mL/min. n	15.69±0.94 34	16.81±1.10 27	18.19±1.70 20	20.02±2.11 18	21.44±1.84 18	20.95±3.49 15	17.38±1.86 14	22.50±1.70 8

Data represented as an average ±SEM.

*P≤0.05

†P≤0.01

‡P≤0.001, by unpaired student's two-tailed t test with Welch's correction.

Table 2:

Echocardiogram analysis of $Adm^{+/+}$ and $Adm^{hi/hi}$ females before and after MI. BPM indicates beats per minutes; CO, cardiac output; d, diastolic; EF, ejection fraction; FS, fractional shortening; IVS, interventricular septal; LV, left ventricle; LVID, left ventricle internal diameter; LVPW, left ventricle posterior wall; and s, systole. Data represented as an average ±SEM.

	Baseline		**4 Days Post LAD**		**10 Days Post LAD**	
	***Adm*$^{+/+}$**	***Adm*$^{hi/hi}$**	***Adm*$^{+/+}$**	***Adm*$^{hi/hi}$**	***Adm*$^{+/+}$**	***Adm*$^{hi/hi}$**
IVS;d mm	1.19±0.07	0.94±0.15	1.22±0.8	1.11±0.18	1.09±0.05	1.23±0.06
IVS;s mm	1.85±0.11	1.60±0.22	1.73±0.16	1.51±0.27	1.51±0.14	1.20 *±0.15
LVID;d mm	2.43±0.18	3.32 *±0.22	3.49±0.13	3.85±0.12	3.72±0.28	4.11±0.29
LVID;s mm	1.20±0.04	1.74±0.35	2.46±0.15	3.04±0.24	2.79±0.21	2.74±0.21
LVPW;d mm	1.05±0.08	1.05±0.12	1.17±0.12	1.17±0.20	1.14±0.11	1.12±0.17
LVPW;s mm	1.65±0.09	1.76±0.19	1.53±0.13	1.41±0.15	1.53±0.13	1.54±0.11
LV Mass mg	93.73±11.98	121.4±23.91	168.2±8.63	183.7±16.17	168.0±15.47	210.0±13.00
LV Mass (Corrected) mg	74.98±9.59	97.14±19.13	134.6±6.91	146.9±12.93	134.4±12.38	168.0±10.40
LV Vol;d µl	21.93±3.99	45.75 *±7.21	51.19±4.41	64.06±4.54	62.07±10.45	76.42±11.40
LV Vol;s µl	3.40±0.35	11.01±5.73	22.17±3.27	37.29±7.04	30.80±5.06	28.72±5.14
EF %	81.02±3.51	78.51±9.09	57.66±3.54	42.87±8.13	48.88±4.80	62.42 *±3.18
FS %	48.89±4.13	48.57±7.73	29.89±2.32	21.22±4.54	24.65±3.07	33.44 *±2.34
Heart Rate BPM	712.2±24.86	620.0±42.30	697.9±12.39	675.1±34.78	711.5±8.06	706.5±4.71
CO (Approx.) mL/min. n	13.21±2.87 7	21.72±3.96 4	20.30±1.71 7	17.79±2.44 4	22.09±4.68 7	33.63±5.29 4

*P≤0.05, by unpaired student's two-tailed t test with Welch's correction.